A High Flux Source of Energetic Oxygen Atoms for Material Degradation Studies

George E. Caledonia,* Robert H. Krech,† and Byron D. Green‡
Physical Sciences Inc., Andover, Massachusetts

A novel technique for generation of a high flux of energetic (nominal ~5 eV) oxygen atoms has been demonstrated in the laboratory. The generation technique involves a laser-induced breakdown of molecular oxygen followed by a rapid expansion of the recombining plasma, resulting in the production of a flux of nearly monoenergetic oxygen atoms. We have developed consistently high velocity streams of oxygen atoms in an evacuated hypersonic nozzle. The oxygen flow is introduced into the nozzle through the mediation of a fast (~100 μs) pulsing valve and broken down with a CO_2 laser. We have measured average oxygen atom velocities of ~5 to 13 km/s with an estimated total production of 10^{18} atoms per pulse over pulse durations of several μs. Although these were single pulse measurements, scaling to a repetitively pulsed device appears straightforward. The O-atom source was used to irradiate sample targets, including Al, Fe, and polyethylene, and target-material-specific radiation was observed above the target surfaces, indicating energetic O-atom induced mass removal.

Introduction

ONE of the most significant observations during the early missions of the Space Shuttle was the degradation and mass loss of certain materials upon exposure to the low Earth orbit environment. For example, Kapton suffered a loss of transparency, paint lost gloss, carbon was removed from surfaces, and silver underwent oxidation.[1-4] As the Shuttle sweeps through its orbit at velocities of 8 km/s, the Earth's natural atmospheric species energetically impact on the Shuttle's ram direction surfaces. At low Earth-orbit Shuttle mission altitudes (230-310 km), the natural atmosphere is dominantly O-atoms. Although the atmosphere is quite variable at these altitudes, a surface at normal incidence to the orbital velocity vector is subjected to O-atom fluxes in the range of 4×10^{14}-2×10^{15} cm^{-2} s^{-1} (Refs. 1-3). These atoms are chemically reactive and are strongly suspected to be the major source of the observed material degradation. Experimental pallets flown on STS-5 and -8 clearly demonstrated the dependence of the degradation on ram atom flux exposure and began to quantify mass losses and changes in various material properties (tensile strength, optical quality) for a host of materials of aerospace interest over a range of material thickness, coatings, temperatures, and reactive fluxes (and exposure times) while on orbit.[2] The STS-8 pallet was exposed to an integrated O-atom flux of 3.5×10^{20} cm^{-2} and the observations revealed that material ranged from quite reactive (e.g., polymeric hydrocarbons, epoxies, urethanes, graphites, osmium, and silver) to relatively inert (e.g., silicons, silicates, fluorides, fluorinated hydrocarbons, oxide pigments, and noble metals). For the most reactive compounds such as Kapton, 10% of surface/O-atom collisions led to mass loss, most probably through chemical reaction.[2,3]

The observations from STS-5 and -8 have laid the groundwork for more detailed measurements planned for a later Shuttle flight—the EOIM-3 measurement program, where mechanisms and O-atom combustion reaction products will be investigated using sophisticated detection techniques. The need for such measurements has been emphasized recently in a study by Leger et al.[5] where it was demonstrated that O-atom material degradation also could have a severe impact on the performance of the Space Station. These observations have led NASA to pursue the development of various material hardening techniques directed to make materials more impervious to the effects of energetic oxygen atoms.

These observations and program directions stress the need for a laboratory facility that can be used to measure/study material degradation due to energetic O-atoms. While the Space Shuttle provides a valuable testbed for such investigations, both the large number of materials/flight conditions to be studied and flight scheduling constraints mandate that the major portion of such studies be performed in a ground facility. For example, important parameters include material composition, material temperature, solar UV exposure, sample stress loading, impact angle of reactive flux, etc.[6,7] Furthermore, issues such as flux dependencies and variations in degradation rates with exposure time[8] also require investigation.

We have conceived and successfully implemented a new approach for the production of large fluxes of energetic oxygen atoms, which draws on years of research in the area of pulsed laser propulsion.[9,10] In this concept, an incoming laser beam is focused into the throat of a nozzle to yield a breakdown in the ejected gas. The resulting high-pressure plasma is characteristic of a detonation wave initiated by a high-power laser-induced breakdown. With a short duration laser pulse, the detonation wave quickly becomes a blast wave, which propagates to the nozzle exit plane, converting all of the high pressure of the gas behind it into a propelling force. The stagnation energy of the laser-produced plasma is converted effectively to velocity of the exhaust gases.

In the experiments described below, we introduce ~10^{-4} g of pure O_2 into an evacuated expansion nozzle using a fast (~100 μs) pulsed molecular valve. The fast switching allows the gas to remain localized within the nozzle while the 10.6 μm CO_2 laser having pulse energy of ~5 J and pulse length of 2.5 μs is focused into the nozzle so as to cause breakdown at the throat. The subsequent laser-initiated detonation wave heats the major portion of the gas within the nozzle during

Presented as Paper 85-7015 at the AIAA Shuttle Environment and Operations Meeting, Houston, TX, Nov. 13-15, 1985; received Jan. 14, 1986; revision received June 10, 1986.

*Vice President Research.
†Principal Scientist.
‡Manager Aerospace Sciences.

the laser pulse time, creating a high temperature plasma. This plasma then expands through a nozzle, tailored to allow electron-ion recombination but not atomic recombination. As the gas expands its temperature and density drop, however, its directed velocity increases correspondingly. Thus a thermally "cold," high energy beam of oxygen atoms is available at the nozzle exit. For example, with 10^{-4} g of gas and 5 J laser pulse, we estimate formation of $\gtrsim 10^{18}$ oxygen atoms with a characteristic energy of 5 eV. For comparison with other sources, if such a device could be pulsed at 1 Hz (easily achieved with available laser devices) and be expanded out of a nozzle with 100 cm^2 base, an average flux of 10^{16} O-atoms/cm^2-s could be maintained on a 100 cm^2 target. The details of our experimental apparatus and observations are provided below.

Experimental Apparatus

A schematic diagram of the apparatus is shown in Fig. 1. The laser is located in an electromagnetic interference (EMI) reducing enclosure approximately 3 m from the test chamber. Two radiometers for time-of-flight velocity measurements are located on the top flange of the vacuum chamber. An optical multichannel analyzer (OMA) spectrograph is positioned at the side of the vacuum chamber to diagnose the atomic oxygen beam.

A Lumonics K-103 TEA laser is used to generate up to 10 J pulses of 10.6 μ radiation. The laser pulse width is 2.5 μs, with approximately one-third of the energy delivered in the first 200 ns (the gain-switched spike). The radiation in the initial spike generates a laser induced breakdown in the high pressure oxygen at the nozzle throat, forming a plasma that continues to absorb the radiation as long as the laser is on.

The laser beam is directed to the test chamber by three gold turning mirrors. A sodium chloride flat between the second and third mirror reflects 8% of the beam to a Lumonics Model 50D calorimeter to monitor the laser energy. A 300 mm focal length barium fluoride lens (35 mm clear aperture), located in a focusing tube at the entrance window, is used to focus the laser beam approximately to a 1 mm diam spot size at the nozzle throat. Accounting for various losses, approximately one half of the laser energy typically is delivered to the focal spot. Peak spike intensity is about 2×10^9 W/cm^2, which is sufficient to cause a rapid breakdown in the gas.

The test chamber is a standard 20 cm diam six-way stainless steel high vacuum cross with Con-Flat flanges (MDC Inc.). The top flange of the chamber has two 5 cm i.d. quick connect O-ring vacuum couplers to allow the insertion of time-of-flight O-atom radiometers into the chamber. The end flange opposite the pulsed valve assembly has a 5 cm O-ring quick connect to allow for positional adjustment of the laser input lens, which is mounted inside a 5 cm o.d. focusing tube. Each side flange has two 5 cm diam quartz view ports for visual and spectroscopic observations. The bottom flange is connected to a 5 cm diffusion pump stack, which provides for an ultimate pressure in the chamber of 3×10^{-5} torr. In operation, the chamber pressure is kept below 1×10^{-4} torr to prevent beam interaction with the background gas.

The pulsed valve/nozzle assembly is shown schematically in Fig. 2. The valve is a Model BV-100V pulsed molecular beam valve from Newport Research Inc. This valve allows the generation of short duration pulses of gas at high flow rates. The valve is operated with a 1 mm i.d. orifice plate, and is bolted directly to a 100 mm long, 20-deg full angle aluminum expansion nozzle with a 1 mm i.d. throat. The nozzle has two flush-mounted pressure transducers with 1 μs response located 43 and 93 mm from the throat. The choked flow rate of the valve/nozzle assembly is 0.19 g of oxygen per s per atmosphere stagnation pressure. In principle, the valve/driver combination can produce gas pulses as short as 100 μs. The device was operated for several thousand pulses with no observable degradation of the aluminum nozzle.

Optical Measurements

Two kinds of optical measurements are conducted to probe the laser processed O-atom beam. The time history of the 777.3 nm atomic oxygen line emission is measured by two identical radiometers mounted on the top flange of the vacuum chamber to determine the beam velocity. The Hammamatsu R406 Photomultiplier tubes are coupled to a 50 mm focal length lens mounted on a 250 mm long by 50 mm diam telescope barrel passing through the flange plate in O-ring quick connect couplers. The field of view of each radiometer is restricted to a 1×10 mm rectangle perpendicular to and across the flow centerline, by positioning a 4×40 mm slit in the image plane of the lens. The radiometers are separated by 7.6 cm and are located 12 and 19.6 cm from the nozzle throat, respectively. They are filtered to observe only 777.3 nm O-atom emission.

Spectral Measurements

Spectral measurements of the laser processed O-atom beam (and target interactions) are obtained using a Princeton Instruments Optical Multichannel Analyzer (OMA) coupled to a 0.275 m Jarrel Ash Mark X spectrograph. The OMA head consists of a 1024 photodiode array with a gated S-20R intensifier. The spectrograph has a 600 line/mm grating blazed at 450 nm. With a 25 μ entrance slit, the measured

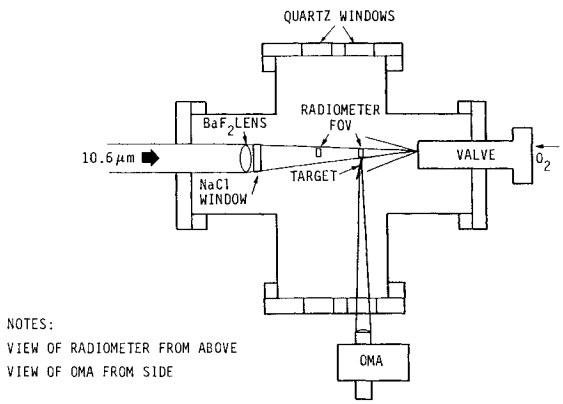

Fig. 1 O-atom experiment schematic.

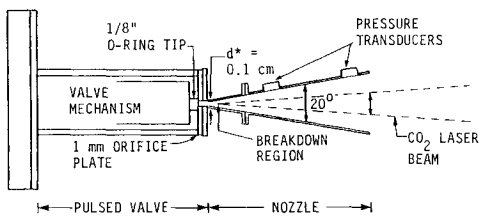

Fig. 2 Schematic of O-atom pulsed valve/nozzle assembly.

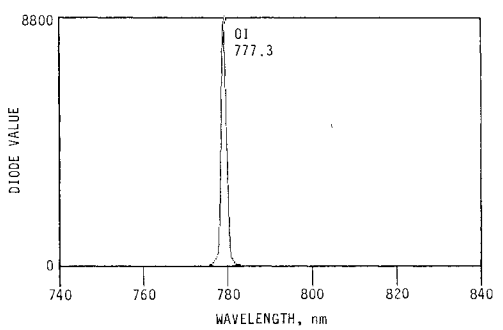

Fig. 3 Red portion of the spectral survey of expanded oxygen plasma.

spectral resolution was 0.6 nm. The optical field of view in the chamber was restricted to a 0.090 by 0.90 cm rectangle centered 2 cm downstream of the nozzle exit by a collecting telescope matched to the f number of the spectrograph (f/4.2) attached to the entrance slit. Colored glass cut-on filters were used to prevent second and higher order spectra from being recorded. Spectra were recorded using the OMA in the gated mode.

O-Atom Source Characterization

Measurements typically were performed with a laser pulse energy of 5 J and an O_2 stagnation pressure of 6⅓ atmospheres. The laser was focused on an approximately 1 mm spot near the nozzle throat. Breakdown in pure O_2 was readily and consistently achieved under these conditions. It is anticipated that breakdown occurred slightly downstream of the nozzle throat, however this postion was not accurately measured.

It was found to be best to flow the O_2 gas for ~ 200 μs prior to applying the laser pulse. This ensured filling the nozzle without increasing the vacuum chamber pressure, which was held to $\sim 10^{-4}$ torr. The nozzle pressure transducers were found to be ineffective due to a combination of electrical noise pick up and high frequency ringing, and thus the key diagnostics for monitoring the heated gas flow were the optical detectors. The OMA was triggered approximately 5 μs after the laser trigger in order to minimize the effect of scattered light from the initial high temperature plasma and was typically gated on for 100 μs.

A number of spectral scans of the radiation from the expanded oxygen plasma were performed over the wavelength range of 400–800 nm. Results were highly reproducible. Two main spectral subsets were observed. The first are the H_λ, H_β, and H_α lines. The impurity radiation later was found to arise from plasma-induced erosion of the hydrocarbon nozzle tip and can be eliminated by appropriate nozzle throat design. The second subset is a series of OI lines, strongly dominated by the transition at 777.3 nm, but also includes transitions at 615.7 and 436.8 nm, among others. These transitions have been identified through a cursory examination of standard tables.[11,12] There are a number of weaker spectral features also seen, many of which have been identified as due to atomic oxygen as seen in electron irradiated air studies.[13] Given that the spectral resolution of the data is 0.6 nm and that many transitions of species such as OII and AlII in addition to OI also fall in this spectral region, no attempt has been made to identify these transitions. Nonetheless, no strong transitions due to OII or Al have been observed and it is clear that the dominant spectral features (with the exception of hydrogen impurity) are due to hot oxygen atoms with no evidence of significant radiation from the nozzle materials or their oxides. There are undoubtedly metastable oxygen atoms in the beam, although their radiation is too weak to be observed. We estimate that they will be present in equilibrium concentrations at the nozzle exhaust temperature.

A typical scan of the red portion of the spectrum is shown in Fig. 3. The only feature observed in this spectral region is the 777.3 nm line. This transition provides an excellent diagnostic for the presence of hot oxygen atoms and thus was used to monitor O-atom velocity. As described above, the two filtered radiometers were positioned to view 12 and 19.6 cm downstream from the nozzle throat. The observed onset of this emission corresponds to the time required for oxygen atoms to reach the monitored point. Thus measurements at different positions can be differentiated to evaluate velocity.

Typical radiometer traces are shown in Fig. 4. Two traces are shown on each oscillogram; the upper trace corresponds to the radiometer positioned at 12 cm and the lower to that positioned at 19.6 cm. Laser onset in each case is marked on the left-hand side of each trace by a small spike on the baseline. The trend is the same in all cases. Radiation is seen first

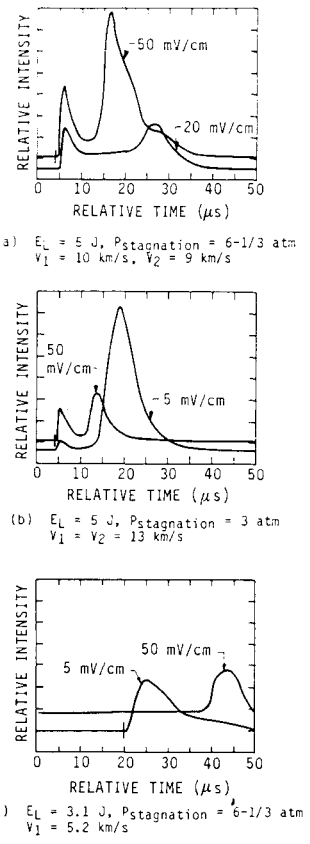

Fig. 4 777.3 nm radiometer histories (timescale is 5 μs per division).

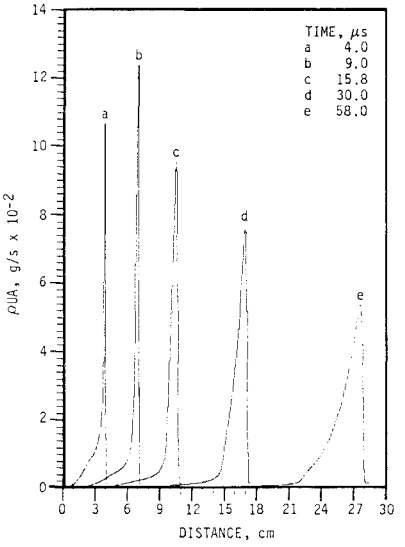

Fig. 5 Predicted profiles of mass flow (gas density * velocity × area) within the nozzle at different times. $E_L = 5$ J, $P_{stagnation} = 6⅓$ atm.

within a few μs of the laser pulse. This radiation occurs much too soon to be from hot gases expanded through the nozzle. Rather it is anticipated that this is due perhaps to either photoexcitation of the ambient gases by the hard UV radiation produced by the oxygen plasma or scattered light from the plasma (recall that the laser pulse width is 2.5 μs). The second sharply rising peak is attributed to the passage of energetic oxygen atoms. This "spike" of radiation typically has a width of 10 μs and is delayed and slightly wider at the downstream location as anticipated.

The characteristic velocity of the oxygen atoms can be defined in several ways. We have chosen an average velocity as defined by the distance from the nozzle throat and the time to reach peak radiation after laser pulse initiation on both radiometers. The values of average velocity are listed in Fig. 4 with the subscripts 1 and 2 referring to the radiometers positioned 12 and 19.6 cm from the nozzle throat, respectively. The important quantity in determining O-atom velocity is the amount of energy deposited per unit mass of gas in the nozzle. The three cases shown in Fig. 4, were chosen to exemplify this variation. In these studies, we have not measured the total energy absorbed but only the total incident laser energy and thus the comparisons can only be qualitative. Nonetheless, the observed trends are as anticipated.

Figure 4a corresponds to ~5 J incident energy into a filled nozzle with a plenum pressure of 6⅓ atm of O_2. Deduced velocities are found to be 9–10 km/s, slightly larger than Shuttle orbital velocities. Figure 4b corresponds to the same laser energy but a plenum pressure of 3 atm. As expected, the velocity is higher in this case, ~13 km/s. Figure 4c corresponds to a reduced laser energy of 3.1 J and a plenum pressure of 6⅓ atm, i.e., the same as Fig. 4a except for a lower laser energy, and here the velocity is reduced to 5 km/s. We note that to first order we expect the velocity to scale as $V\alpha\sqrt{E/\Delta m}$, where E is the laser energy absorbed and Δm is the mass processed. The observations shown in Fig. 4, which are highly reproducible, are clearly in qualitative agreement with such scaling.

A theoretical prediction has been provided for comparison with the data using a validated code that can predict the unsteady expansion of the heated plasma.[14] The nozzle expansion is modeled by quasi-one-dimensional flow in a variable area nozzle. The physical phenomena included in the model are 1) conservation of mass, momentum, and energy; 2) chemical equilibrium of the flowing gas; and 3) heat addition by absorption of laser energy. The calculation was initiated by assuming one-third of the laser energy (the gain-switched spike) was absorbed instantaneously by the gas within the first cm from the nozzle throat. The remaining laser energy was then modeled as being absorbed through inverse Bremsstrahlung mechanisms occurring within the fluid dynamically active plasma. The area distribution specified, corresponded to that of the nozzle used in the experiments, except that the length was taken as 20 cm. The code thermodynamic data is sufficient to characterize accurately oxygen plasmas up to triply ionized states.

The calculation was performed for a CO_2 laser pulse energy of 5 J and a plenum pressure of 6⅓ atm, corresponding to the case shown in Fig. 4a. The predicted fluid dynamical behavior is displayed in Fig. 5, which exhibits "snapshots" of the profile of mass flow rate in the nozzle as a function of distance at different flow times. What is depicted clearly is a narrow "slug" of gas moving rapidly down the nozzle. Predicted profiles of mass per unit length in the nozzle have very similar shapes, demonstrating that the major portion of the heated gas at any one time is moving at a characteristic velocity with very little spread, ideal for simulation studies of Shuttle material degradation.

Similar profiles of atom velocity vs distance at different flow times are shown in Fig. 6. These predictions are for the instantaneous local velocity distribution and are not to be confused with the average velocities deduced from the radiometer traces. The blips observed in the profiles are most probably a numerical artifact of the code and should be ignored. Note that the velocity profiles are quite broad. Nonetheless, from comparison with Fig. 5, it can be seen that the velocity variation over the axial range of the gas pulse is predicted to be very small, ideal for the present beam application. The predicted gas behavior is characteristic of that associated with a blast wave. Although the gas velocity scales inversely with distance from the source, most of the mass is at the wave front, and thus the resulting atomic beam is near monoenergetic.

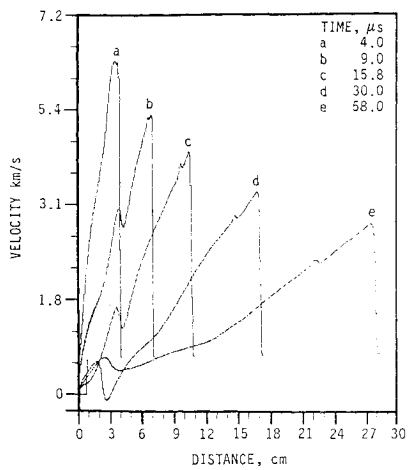

Fig. 6 Predicted profiles of gas velocity for the conditions of Fig. 5.

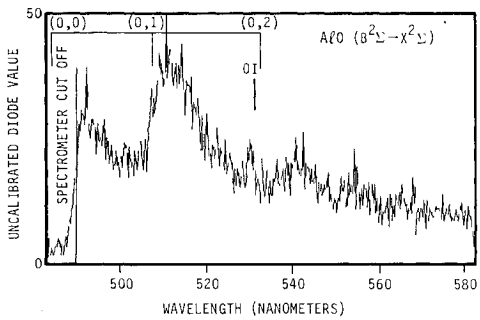

Fig. 7 Observed emission over ALCLAD 7075 target (average of four shots) (E_L ~5 J, $P_{stagnation}$ = 6⅓ atm).

The calculations can be compared only with the data out of the nozzle at 10 cm. This is because the code assumes that the flow continues to ingest gas at larger distances and thus slows down. In reality, the heated gases expand into near vacuum at the nozzle exhaust and should remain at near constant velocity beyond that point. Although the model predictions of gas flow are similar to the observations, the predicted velocities are approximately 30% lower than the measured values. It may be that the nozzle was not uniformly filled during the experiments. In the future, time-of-flight mass spectrometry will be used to characterize the beam velocity.

In summary, we have demonstrated the ability to produce high fluxes of approximately monoenergetic oxygen atoms at velocities comparable to those of interest to low Earth orbit. The actual O-atom flux has not been measured but is estimated from computer predictions to correspond to number densities of ~10^{18} per pulse. Beam conditions appear readily scalable with nozzle pressure and laser energy, and extension to a repetitively pulsed device is straightforward. It is clear that the beam has only been crudely characterized to date and that an expanded system will require more sophisticated diagnostics.

Material Degradation Studies

Once the O-atom source had been characterized, a limited number of target irradiation observations were performed. The object of these was not to monitor mass loss or surface modification but merely to study the spectral signatures above irradiated surfaces in order to identify spectral

features peculiar to the O-atom/material interaction. To this end, small targets of aluminum and iron were introduced into the test chamber at a distance 17.1 cm downstream of the nozzle throat and irradiated with oxygen atoms generated under the $E_L = 5$ J, $P_{\text{stagnation}} = 6\frac{1}{3}$ atm conditions. The radiation above the surfaces of these targets was monitored with the OMA instrument in order to identify spectral features due to, for instance, metal oxides, which would provide evidence of oxygen atom induced material degradation. The OMA was positioned to look at the target at a ~10 deg grazing angle.

The first measurements were made above an aluminum target, ALCLAD 7075. The observed spectrum was compared directly to the measurement performed in the absence of the target and many of the spectral features previously observed were also seen above the aluminum target. The relative intensities are different, however, suggesting selective quenching/reaction on the surface. Several new spectral features appear, which remain to be identified.

The (0,0) bandhead of the AlO green band is unfortunately near coincident with the strong H_β transition. Radiation to the red of this latter transition was monitored and the results are shown in Fig. 7. Band head positions of the $(0,v')$ sequences are also designated[15] and, although the signal is quite noisy, it does appear that radiation from AlO has been observed. More careful and detailed measurements will be required to verify this.

Similar measurements were performed with a target of generic cold-rolled steel. Again the H_λ and H_β transitions are seen as well as the feature at 431 nm. Many of the other transitions observed over the aluminum target and in heated oxygen flow were not seen here however. A search was made for the FeO orange bands which fall between 530–680 nm[13]; although there was some evidence of banded structure in the spectra, the FeO bands could not be positively identified.

A polyethylene sample also was irradiated. The sample was supplied by the Jet Propulsion Lab and was from the same block of material as that flown on STS-8.[3] The polyethylene was irradiated with several hundred oxygen-atom pulses and then examined by Electron Spectroscopy for Chemical Analysis (ESCA). The measured oxygen surface enrichment of the polyethylene was very similar to that observed in post-flight analysis of the same flown on STS-8.[16] Portions of the sample within the test chamber, but not struck by the O-atom beam, showed no enhancement. The irradiaiton level was insufficient to measure mass loss.

Other polymeric targets were also examined briefly. Strong radiative features corresponding to electronic bands of CN and OH were observed. No quantitative evaluation of this data has been performed.

These target studies were necessarily quick surveys, however, it is clear that target interactions provide for significantly varying spectral signatures with some spectral features indicative of mass removal. It is clear that spectra averaged over many O-atom pulses should provide information on the kinetic mechanisms responsible for mass removal which could be used in conjunction with mass loss and surface modification observations for mechanistic interpretations of oxygen atom material interactions. Furthermore, there has been considerable discussion of observed glows over spacecraft surfaces.[4] It is clear that chemical reactions between ambient oxygen atoms and spacecraft surfaces can produce volatile species in excited states, thus introducing material specific radiation signatures. Such effects undoubtedly occur but have not yet been quantified in Space Shuttle observations. The present facility can be directly applied to study such signatures through the ultraviolet to the infrared.

Acknowledgments

This research was funded by NASA under Contract NAS7-938 and monitored by the Jet Propulsion Laboratory. Dr. D. I. Rosen of Physical Sciences Inc. provided helpful discussions and insight throughout the course of the program. Dr. N. Kemp of Physical Sciences Inc. provided the computer model calculations.

References

[1]Leger, L. J., Spiker, I. K., Kuminecz, J. F., and Visentine, J. T., "STS Flight 5 LEO Effects Experiments—Background Description and Thin Film Results," AIAA Paper 83-2631, Oct. 1983.

[2]Leger, L. J., Visentine, J. T., and Kuminecz, J. F., "Low Earth Orbit Atomic Oxygen Effects on Surfaces," AIAA Paper 84-0548, Jan. 1984.

[3]Visentine, J. T., Leger, L. J., Kuminecz, J. F., and Spiker, I. K., "STS-8 Atomic Oxygen Effects Experiment," AIAA Paper 85-0415, Jan. 1985.

[4]Green, B. D., Caledonia, G. E., and Wilkerson, T. D., "The Shuttle Environment: Gases, Particulates and Glow," *Journal of Spacecraft and Rockets*, Vol. 22, Sept.-Oct. 1985, pp. 500–511.

[5]Leger, L. J., Visentine, J. T., and Schliesing, J. A., "A Consideration of Atomic Oxygen Interactions with Space Station," AIAA Paper 85-0476, Jan. 1985.

[6]Hall, D. F. and Steward, T. B., "Photo-Enhanced Spacecraft Contamination Deposition," AIAA Paper 85-0953, June 1985.

[7]Peterson, R. V., Hanna, W. D., and Mertz, L. O., "Results of Oxygen Atom Interaction with Kevlar and Fiberglass Fabrics on STS-8," AIAA Paper 85-0990, June 1985.

[8]Knopf, P. W., Martin, R. J., McCargo, M., and Dammann, R. E., "Correlation of Laboratory and Flight Data for the Effects of the Atomic Oxygen on Polymeric Materials," AIAA Paper 85-1066, June 1985.

[9]Simons, G. A. and Pirri, A. N., "The Fluid Mechanics of Pulsed Laser Propulsion," *AIAA Journal*, Vol. 15, June 1977, pp. 835–842.

[10]Rosen, D. I., Pirri, A. N., Weiss, R. F., and Kemp, N. H., "Repetitively Pulsed Laser Propulsion: Needed Research," *Progress in Astronautics and Aeronautics*, edited by L. H. Caveny, Vol. 89, 1984, pp. 95–108.

[11]Weise, W. L., Smith, M. W., and Glennon B. M., "Atomic Transition Probabilities, Vol. I, Hydrogen Through Neon," NSRDS-NBS 4, Washington, DC, 1966.

[12]Bashkin, S. and Stoner, J. O. Jr., "Atomic Energy-Level and Grotrian Diagrams, Vol. I, Hydrogen I—Phosphorous XV," North-Holland Publishing Co., Amsterdam, the Netherlands, 1978. .

[13]Blumberg, W. A. M., Wolnik, S. J., Green, B. D., and Caledonia, G. E., "Formation and Relaxation of Highly Excited Atomic Oxygen," EOS 65, SA11-12, 1984.

[14]Kemp, N. H., "Computer Simulation of the Non-Steady Flow of a Real Gas with Laser Energy Absorption," AIAA Paper 84-1568, June 1984.

[15]Pearse, R. W. B. and Gaydon, A. G., *The Identification of Molecular Spectra*, Chapman and Hall Ltd., London, 1963, p. 63.

[16]Coulter, D., Jet Propulsion Laboratory, Pasadena, CA, private communication, 1985.